Inorganic Chemistry

Article

pubs.acs.org/IC

Novel Alkali Earth Borohydride $Sr(BH_4)_2$ and Borohydride-Chloride $Sr(BH_4)Cl$

D. B. Ravnsbæk,*[,†,‡] E. A. Nickels,[§,∥] R. Černý,[#] C. H. Olesen,[‡] W. I. F. David,[§,∥] P. P. Edwards,[§] Y. Filinchuk,[⊥] and T. R. Jensen[‡]

[†]Department of Material Science and Engineering, Massachusetts Institute of Technology, 77 Massachusetts Avenue, Cambridge, Massachusetts 02139, United States

[‡]Center for Materials Crystallography (CMC), Interdisciplinary Nanoscience Center (iNANO), and Department of Chemistry, University of Aarhus, Langelandsgade 140, 8000 Aarhus C, Denmark

[§]Inorganic Chemistry Laboratory, University of Oxford, South Parks Road, Oxford, OX1 3QR, United Kingdom

[∥]ISIS Facility, Rutherford Appleton Laboratory, Chilton, Didcot, Oxon, OX11 0QX, United Kingdom

[⊥]Institute of Condensed Matter and Nanosciences, Université Catholique de Louvain, Place L. Pasteur, B-1348, Louvain-la-Neuve, Belgium

[#]Laboratory of Crystallography, Department of Condensed Matter Physics, University of Geneva, 1211 Geneva, Switzerland

Supporting Information

ABSTRACT: Two novel alkali earth borohydrides, $Sr(BH_4)_2$ and $Sr(BH_4)Cl$, have been synthesized and investigated by in-situ synchrotron radiation powder X-ray diffraction (SR-PXD) and Raman spectroscopy. Strontium borohydride, $Sr(BH_4)_2$, was synthesized via a metathesis reaction between $LiBH_4$ and $SrCl_2$ by two complementary methods, i.e., solvent-mediated and mechanochemical synthesis, while $Sr(BH_4)Cl$ was obtained from mechanochemical synthesis, i.e., ball milling. $Sr(BH_4)_2$ crystallizes in the orthorhombic crystal system, a = 6.97833(9) Å, b = 8.39651(11) Å, and c = 7.55931(10) Å (V = 442.927(10) Å^3) at RT with space group symmetry *Pbcn*. The compound crystallizes in α-PbO_2 structure type and is built from half-occupied brucite-like layers of slightly distorted $[Sr(BH_4)_6]$ octahedra stacked in the a-axis direction. Strontium borohydride chloride, $Sr(BH_4)Cl$, is a stoichiometric, ordered compound, which also crystallizes in the orthorhombic crystal system, a = 10.8873(8) Å, b = 4.6035(3) Å, and c = 7.4398(6) Å (V = 372.91(3) Å^3) at RT, with space group symmetry *Pnma* and structure type $Sr(OH)_2$. $Sr(BH_4)Cl$ dissociates into $Sr(BH_4)_2$ and $SrCl_2$ at ∼170 °C, while $Sr(BH_4)_2$ is found to decompose in multiple steps between 270 and 465 °C with formation of several decomposition products, e.g., SrB_6. Furthermore, partly characterized new compounds are also reported here, e.g., a solvate of $Sr(BH_4)_2$ and two Li−Sr−BH_4 compounds.

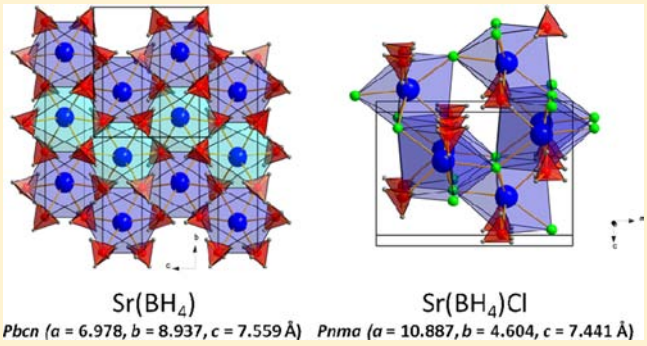

INTRODUCTION

Hydrogen is widely recognized as a potential energy carrier in a future sustainable and reliable energy system. However, development of safe, compact, robust, and efficient means of hydrogen storage is a major challenge in the realization of a future hydrogen-based energy system.[1,2] Borohydride-based materials have received much attention during the past decade as potential hydrogen storage materials due to their high hydrogen densities,[3,4] e.g., gravimetric density, ρ_m = 18.5 wt % H_2, and volumetric density, ρ_V = 121 g H_2/L for $LiBH_4$,[5] and tunable decomposition temperatures,[6,7] e.g., T_{dec} = 585 and 80 °C for KBH_4 and $KCd(BH_4)_3$, respectively.[3,6]

Recently, a wide range of novel borohydrides have been prepared combining different metals, filling the gap between the thermally stable alkali and the unstable transition metal borohydrides.[4,8−12] These studies have revealed an interesting structural diversity within this class of material and bonding in metal borohydrides that can range from ionic to partly covalent or exhibit a combination of both, resulting in complex structures. In bimetallic borohydrides, metal atoms of the more electronegative elements and BH_4 groups tend to form partly covalent complex anions, such as $[Zn_2(BH_4)_5]^-$ and $[Sc(BH_4)_4]^-$ in $MZn_2(BH_4)_5$ (M = Li or Na) and $MSc(BH_4)_4$ (M = Li, Na or K), respectively.[13−18]

Furthermore, the monometallic alkali earth metal borohydrides, $Mg(BH_4)_2$ and $Ca(BH_4)_2$, have been widely investigated due to their high hydrogen contents (14.9 and 11.6 wt %, respectively) and rich crystal polymorphism, i.e., four polymorphs are known for both compounds.[4,19−22] Recently,

Received: April 8, 2013
Published: September 19, 2013

Table 1. Reaction Products Observed by SR-PXD Measured at RT for Sample Prepared by Solvent-Mediated (SM) Synthesis (Sample A) and Mechanochemical Synthesis, i.e., Ball Milling (BM) (samples B−E)

	SM, sample A			
starting composition $LiBH_4$:$NaBH_4$:$SrCl_2$	3:1.5:1			
reaction products	$Sr(BH_4)_2$, **1**,[a] LiCl			
	BM			
	sample B	sample C	sample D	sample E
starting composition $LiBH_4$:$SrCl_2$	1:1	2:1	3:1	4:1
reaction products	$Sr(BH_4)Cl$, $Sr(BH_4)_2$,[b] LiCl, $SrCl_2$	$Sr(BH_4)_2$, **2** ($P2/m$), **3** ($P2_1/m$), LiCl, $SrCl_2$	$Sr(BH_4)_2$,[b] **3** ($P2_1/m$), LiCl, $SrCl_2$	**3** ($P2_1/m$), LiCl, $SrCl_2$

[a]Orthorhombic unit cell (see text). [b]Observed in small amounts.

two novel magnesium borohydride polymorphs were discovered, γ- and δ-$Mg(BH_4)_2$.[20,21] The former, γ-$Mg(BH_4)_2$, represents a novel nanoporous zeolite-type framework structure, which has the capability to absorb small gas molecules, while the dense δ-$Mg(BH_4)_2$ polymorph has the second highest volumetric hydrogen density ρ_V = 147 g H_2/L among all known hydrides (slightly lower than $\rho_V(Mg_2FeH_6)$ = 150 g H_2/L), which is more than twice that of liquid hydrogen, $\rho_V(H_2)$ = 71 g/L.

Hence, the synthesis and characterization of strontium borohydride is of wide interest. Here we report on the synthesis, characterization, and thermal decomposition of two novel alkali earth borohydrides $Sr(BH_4)_2$ and $Sr(BH_4)Cl$, synthesized by two complementary methods, i.e., solvent-mediated and mechanochemical synthesis. The novel compounds are studied by in-situ synchrotron radiation powder X-ray diffraction (SR-PXD) and Raman spectroscopy.

EXPERIMENTAL SECTION

Synthesis. Two synthesis methods were employed aiming at preparing $Sr(BH_4)_2$, i.e., solvent-mediated synthesis and mechanochemical synthesis.[23,24]

Sample A (prepared at University of Oxford) was prepared according to the method used by Mikheeva et al.[25] Within an argon-filled glovebox (O_2 < 20 ppm) 2.75 g of strontium chloride, $SrCl_2$ (99.99%, Sigma Aldrich), 1 g of sodium borohydride, $NaBH_4$ (98%, Sigma Aldrich), and 1.15 g of lithium borohydride, $LiBH_4$ (>95.0%, Sigma Aldrich), were loaded into a Schlenk flask (see Table 1). The flask was sealed, removed from the glovebox, and attached to a nitrogen Schlenk line. Anhydrous tetrahydrofuran (THF) was added to the flask, and the solution was stirred at room temperature (RT) under nitrogen for 2 days. The solution was filtered, and the filtrate was concentrated by evaporation under reduced pressure. Diethyl ether (Et_2O) was added to the filtrate, causing a white precipitate to form. The precipitate was filtered and dried under dynamic vacuum, initially at RT via the Schlenk line before being transferred to a vertical tube furnace and heated to 70 °C for 1 h and 100 °C for a further 30 min.

For samples B−E (prepared at Aarhus University) anhydrous $SrCl_2$ (≥99.99%, Sigma Aldrich) and $LiBH_4$ (≥95.0%, Sigma Aldrich) were combined in molar ratios of $LiBH_4$:$SrCl_2$ of 1:1, 2:1, 3:1, and 4:1 (see Table 1) and ball milled in a Fritch Pulverisette No. 4 using 80 mL of tungsten carbide steel containers and an approximate 1:35 weight ratio of sample to 10 mm tungsten carbide steel balls. All samples were ball milled using the same procedure, i.e., high-energy ball milling under inert conditions (argon atmosphere) comprised of 60 times 2 min of milling each intervened by 2 min breaks to avoid heating of the sample. Preparation and manipulation of all samples were performed in an argon-filled glovebox with a circulation purifier ($p(O_2, H_2O)$ < 1 ppm).

In-Situ Time-Resolved Synchrotron Powder Diffraction. For sample A high-resolution (HR) in-situ time-resolved synchrotron radiation powder X-ray diffraction (SR-PXD) data were collected at the beamline ID31, the European Synchrotron Radiation Facility (ESRF) in Grenoble, France, using a wavelength and step size of 0.799888 Å and 0.003°, respectively. The sample was mounted in a sealed glass capillary with an outer diameter (o.d.) of 1 mm. A variable-temperature experiment was carried out collecting data at 25 °C intervals from 25 to 375 °C heating with a hot air blower. To avoid radiation damage during the variable-temperature experiment, the capillary containing the sample was moved 2 mm along its axis between each scan so that each data set was collected from a heated but not previously exposed part of the sample. Diffraction patterns between 200 and 375 °C were collected in a second experiment using a new sample.

For samples B−E SR-PXD data were collected at the Swiss-Norwegian Beamlines (SNBL), ESRF. Data were collected using a MAR345 image plate detector and radiation with selected wavelengths of 0.700130 and 0.832117 Å. Samples were mounted in glass capillaries (o.d. 0.5 mm) sealed with glue. The capillary was oscillated by 60° during exposure to the X-ray beam for 60 s, followed by readout for ∼83 s. During the variable-temperature experiments samples were heated from RT to 223 or 500 °C at selected heating rates ranging from 1 to 4 °C/min. Temperature was controlled with an Oxford Cryostream 700+ or a hot air blower. Notice that data sets measured using a selected wavelength below λ = 0.7699 Å unfortunately suffer from high background due to the excitation of Kα Sr absorption edge.

Furthermore, a SR-PXD data set has been collected for sample C at the beamline I711 of the synchrotron MAX II, Lund, Sweden, in the research laboratory MAX-Lab. Data were collected using a MAR165 CCD detector system and selected wavelength of 1.0970 Å. The CCD camera exposure time was 30 s. The sample cell was specially developed for studies of gas/solid reactions and allows high pressure and temperature to be applied.[26] Powdered samples were mounted in a sapphire single-crystal tube (o.d. 1.09 mm, i.d. 0.79 mm) in an argon-filled glovebox ($p(O_2, H_2O)$ < 1 ppm). The sample holder was sealed inside the glovebox. Temperature was controlled with a thermocouple placed in the sapphire tube ∼1 mm from the sample. Samples were typically heated from RT to 500 °C with a selected heating rate of 5 °C/min.

All obtained raw images were transformed to 2D powder diffraction patterns using the FIT2D program,[27] which was also used to remove diffraction spots from the single-crystal sapphire tube used as sample holder.

Structure Solution and Refinement. The structure of $Sr(BH_4)_2$ was solved simultaneously and independently from SR-PXD data measured for the sample prepared by solvent-mediated synthesis (sample A) and those prepared by mechanochemical synthesis (samples B−E) yielding the same solution.

The structure of $Sr(BH_4)_2$ was solved from the HR SR-PXD data measured at 175 °C for sample A, in which only diffraction from $Sr(BH_4)_2$ (98 wt %) and a small amount of LiCl (2 wt %) is observed. Peaks were indexed to the orthorhombic *Pbna* space group using the program DASH.[28] Subsequent analysis using TOPAS[29] confirmed this solution. However, manual comparison of the observed reflections to

the reflection conditions of the more favorable space groups identified by TOPAS analysis (*Pbna*, *Pbcn*, *Pbca*, and *Pnma*) indicated that the space group *Pbcn* could be more favorable. A comparison of the indexed cell volume ($V \approx 456$ Å^3) with volume per formula unit of α- and β-$Mg(BH_4)_2$ (V/Z = 114.5(3) and 117.9(5) Å^3)[30,31] as well as α- and β-$Ca(BH_4)_2$ (V/Z = 108.269(1) and 105.3497(1) Å^3)[32,33] suggested $Z = 4$ for $Sr(BH_4)_2$. Using TOPAS, atoms were placed on the special crystallographic positions with multiplicity of four according to the International Tables for Crystallography.[34] The 4*c* site (0, *y*, 0.25) refined to a single occupancy of a strontium atom. The 4*a* (0, 0, 0) and 4*b* (0, 0.5, 0) sites refined to zero occupancy. A boron atom was subsequently inserted into the unit cell at random coordinates with the site occupancy fixed to unity. The position of the boron atom was refined in order to find a reasonable position resulting in the best fit to the data. Hydrogen atoms were added using tetrahedral rigid bodies centered on the boron atoms and fixed B−H distances of 1.12 Å. The resulting structure contains one Sr atom (position 4*c*) and one BH_4 group (general position 8*d*) in the asymmetric unit. BH_4 tetrahedra were allowed to rotate freely; however, accurate hydrogen positions could not be determined. Final refinement was performed using the Rietveld method in the program GSAS.[35] Incorporation of 9.8 mol % Cl on the BH_4 site is detected. This was modeled by introducing a Cl atom on the position of B and constraining the sum of their occupancies to 1. Refined unit cell parameters for $Sr(BH_4)_2$ (space group *Pbcn*) at 175 °C are a = 7.02444(8) Å, b = 8.50969(10) Å, and c = 7.62214(9) Å (V = 455.620(9) Å^3, $Z = 4$). Agreement factors are $\chi^2 = 1.28$, $R_{exp} = 7.71\%$, $R_{wp} = 9.89\%$, and $R_p = 8.28\%$ (see Figure 1). Complete crystallographic information is shown in Table 2, while atomic coordinates can be found in Table S1, Supporting Information. Subsequently, unit cell parameters were refined from data measured for sample A at RT: a = 6.97833(9) Å, b = 8.39651(11) Å, and c = 7.55931(10) Å (V = 442.927(10) Å^3). Due to the presence of an unknown compound (denoted **1**), atomic positions in $Sr(BH_4)_2$ were not refined at RT.

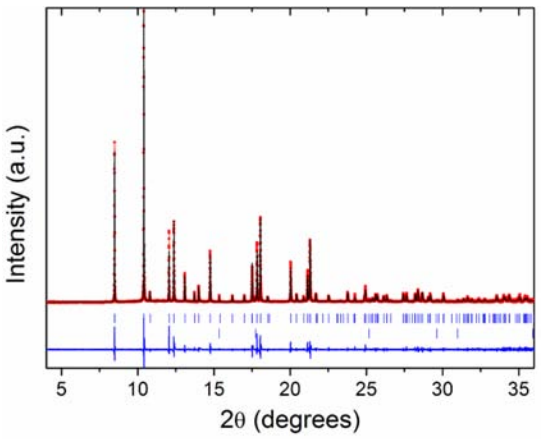

Figure 1. Rietveld plot for sample prepared by solvent-mediated synthesis (sample A) containing $Sr(BH_4)_2$ (upper blue marks) and small amounts of LiCl (lower blue marks). Data are measured at 175 °C (λ = 0.799888 Å): observed data (Y_{obs}, red curve), Rietveld refinement profile (Y_{calc}, black curve), and difference plot ($Y_{obs} - Y_{calcd}$, blue curve).

Simultaneously, the structure of $Sr(BH_4)_2$ was solved from SR-PXD data measured for the ball-milled sample of $LiBH_4$–$SrCl_2$ in a molar ratio of 2:1 (sample C) at 227 °C. The 17 observed peaks assigned to $Sr(BH_4)_2$ were indexed with DICVOL04[36] in an orthorhombic lattice with unit cell parameters (values from final Rietveld refinement of the data measured at 230 °C) a = 6.9415(11) Å, b = 8.3770(14) Å, and c = 7.5532(11) Å (V = 439.21(12) Å^3). Systematic absences led to space group *Pbcn*, and the structure was solved with the direct space method program FOX[37] and subsequently refined with the Rietveld method using the FULLPROF program.[38] The symmetry of the refined structure has been checked with the routine ADDSYM in the program PLATON,[39] and the space group *Pbcn* was confirmed. The structure was solved with the BH_4 group as a rigid ideal tetrahedron with one common B−H distance of 1.13 Å. The orientation of the BH_4 group was not refined; however, it was optimized in FOX by two antibump distance restraints (Sr−H = 2.5 Å and H−H = 2.5 Å) to minimize the repulsive H−H interactions, and only the position of BH_4 was refined in the Rietveld refinement. B and H positions refined to 0.81(3) occupancy, completed by 0.19(3) chlorine occupancy on the B site. Two displacement parameters (one for Sr and the other for the BH_4 group) have been refined isotropically. The impurities LiCl and $SrCl_2$ have been refined with their lattice parameters and isotropic displacement parameters. The profile function has been modeled for each phase by an independent pseudo-Voigt function. Agreement factors are R_{wp} (not corrected for background) = 0.558%, R_{wp} (corrected for background) = 5.47%, R_{Bragg} ($Sr(BH_4)_2$) = 2.57%, and χ^2 = 876. Crystallographic information and atomic coordinates can be found in Table S2, Supporting Information.

SR-PXD data measured at RT for the ball-milled sample of $LiBH_4$–$SrCl_2$ in a molar ratio of 1:1 (sample B) was used for structure solution of the novel ordered borohydride/chloride $Sr(BH_4)Cl$. The structure solution procedure was similar to that for $Sr(BH_4)_2$ using 19 peaks for indexing, giving an orthorhombic lattice with unit cell parameters from the final Rietveld refinement a = 10.8873(5) Å, b = 4.6036(2) Å, and c = 7.4407(4) Å (V = 372.91(3) Å^3). The systematic absences suggested space group *Pnma* or its noncentrosymetric subgroup $Pn2_1a$. The structure was solved in the first of these two possible space groups. The resulting structure contains one Sr atom (position 4*c*), one BH_4 group (position 4*c*), and one chlorine atom (position 4*c*) in the asymmetric unit. B and H positions refined to 0.932(7) occupancy, completed by 0.068(7) chlorine occupancy on the B site. As an impurity also $Sr(BH_4)_2$ phase (5.6(3) wt%) was observed and refined with the structural model fixed to that from sample C. Agreement factors are R_{wp} (not corrected for background) = 0.38%, R_{wp} (corrected for background) = 4.39%, χ^2 = 373, and R_{Bragg} ($Sr(BH_4)Cl$) = 9.95%. Crystallographic information is shown in Table 2, while atomic coordinates can be found in Table S3, Supporting Information. The high values of χ^2 (for samples B and C) reflect mainly the extremely high counting statistics of the powder diffraction data obtained from modern 2D detectors.

Raman Spectroscopy. Room-temperature Raman spectra were recorded on a Jobin Yvon Dilor Labram 300 confocal spectrometer, fitted with an Olympus microscope using the 10-fold magnification objective. A 20 mW He−Ne laser (633 nm) was used. The spectrometer is fitted with an 1800 L/mm (lines per mm) grating which gives a resolution ranging from 1.0 cm^{-1} at 200 cm^{-1} to 0.5 cm^{-1} at 3600 cm^{-1}. The spectrometer was calibrated with a silicon standard, and the sharp Raman shifts are accurate to ±2 cm^{-1}. Samples were contained inside melting point tubes which were loaded within an argon-filled glovebox and temporarily sealed with vacuum grease before being removed from the glovebox and flame sealed.

RESULTS AND DISCUSSION

Synthesis and Initial Phase Analysis. SR-PXD data for the sample prepared by solvent-mediated synthesis (sample A) show two sets of Bragg peaks, one of which is assigned to $Sr(BH_4)_2$, while the other originates from an unidentified compound, denoted **1** (see Figure 2 and Table 1). Furthermore, a small amount of LiCl is observed. This indicates that the following reactions occur during synthesis (eqs 1 and 2).

$$2MBH_4(THF) + SrCl_2(THF) \rightarrow Sr(BH_4)_2(THF) + 2MCl(s) \quad M = Li \text{ or } Na \tag{1}$$

$$Sr(BH_4)_2(THF) \xrightarrow{Et_2O} Sr(BH_4)_2(s) \tag{2}$$

dx.doi.org/10.1021/ic400862s | Inorg. Chem. 2013, 52, 10877−10885

Table 2. Structural Data Extracted by Rietveld Refinement of SR-PXD Data Measured at RT along with the Hydrogen Content for $Sr(BH_4)_2$ (Sample A) and $Sr(BH_4)Cl$ (Sample B)

	$Sr(BH_4)_2$	$Sr(BH_4)Cl$
space group	*Pbcn*	*Pnma*
structure type	α-PbO_2	$Sr(OH)_2$
a (Å)	6.97833(9)	10.8873(5)
b (Å)	8.39651(11)	4.6036(2)
c (Å)	7.55931(10)	7.4407(4)
Sr−B (Å)	2.96(3)−3.12(3)	2.705(2)−3.109(4)
Sr−Cl (Å)		2.965(3)−3.092(8)
B−Sr−B (deg)	83.7(7)−97.3(7) 169.2(7)−173.9(7)	115.233(2)−116.630(1)
Sr−B−Sr (deg)	96.3(7)−129.9(9)	110.403(2)
Z	4	4
V/*Z* (Å^3)	110.73(10)	93.225(7)
ρ (g cm^{-3})	1.80	2.45
ρ_v (H_2) (kg H_2 m^{-3})	123.1	71.8
ρ_m (H_2) (wt %)	6.85	2.92

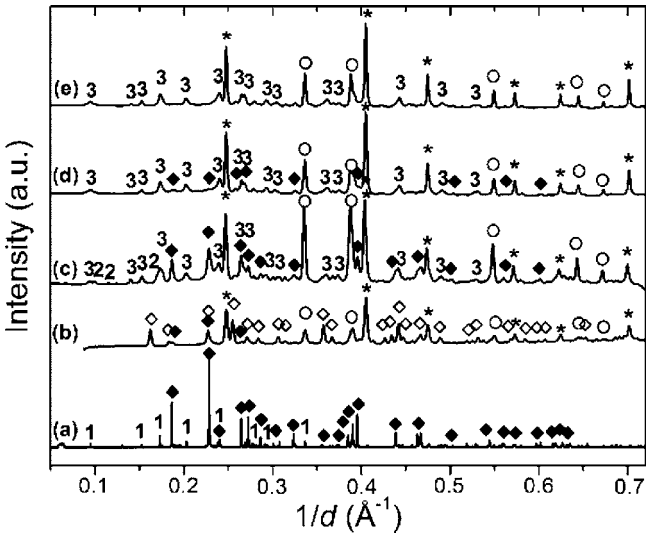

Figure 2. SR-PXD data measured at RT for (a) sample prepared by solvent-mediated synthesis (sample A, λ = 0.799888 Å) and ball-milled samples of $LiBH_4$−$SrCl_2$ in molar composition (b) 1:1 (sample B, λ = 0.700130 Å), (c) 2:1 (sample C, λ = 0.832117 Å), (d) 3:1 (sample D, λ = 0.796201 Å), and (e) 4:1 (sample E, λ = 0.796201 Å). Symbols: (◊) $Sr(BH_4)Cl$ (♦) $Sr(BH_4)_2$, (○) LiCl, (*) $SrCl_2$, while **1**, **2**, and **3** correspond to the unknown compounds described in the text.

Even though both $LiBH_4$ and $NaBH_4$ were used as starting materials for the solvent-mediated synthesis no NaCl was observed by SR-PXD. This suggests either that $NaBH_4$ did not participate in reaction eq 1 to a significant extent or that NaCl formed in the metathesis reaction did not precipitate during addition of diethyl ether.

The unidentified compound, **1**, might be a strontium borohydride solvate, i.e., $Sr(BH_4)_2{\cdot}n(Et_2O)$ or $Sr(BH_4)_2{\cdot}n$THF, remaining after removing the solvent. The unit cell of **1** has been indexed as orthorhombic with *a* = 21.0792(6) Å, *b* = 6.8986(2 Å), *c* = 4.51839(11) Å, and *V* = 657.04(3) Å^3. Bremer et al. reported unit cell parameters for $Sr(BH_4)_2{\cdot}2$THF of *a* = 4.405(1) Å, *b* = 7.997(2) Å, and *c* = 18.826(5) Å,[40] suggesting that **1** may be $Sr(BH_4)_2{\cdot}n(Et_2O)$. However, it has not been possible to solve the structure of **1** from the data obtained in this study.

For the ball-milled sample of $LiBH_4$−$SrCl_2$ in a molar ratio of 1:1 (sample B), SR-PXD data measured at RT show diffraction from two novel strontium borohydrides, $Sr(BH_4)_2$ and $Sr(BH_4)Cl$, as well as LiCl and unreacted $SrCl_2$ (see Table 1 and Figure 2). The weight fractions extracted from Rietveld refinement reveal that the sample consists of 27.2(6) mol % $Sr(BH_4)Cl$ (40.2(9) wt%), while only 4.5(2) mol % $Sr(BH_4)_2$ (5.7(3) wt%) is observed. This suggests that the dominant reaction occurring for this sample composition during mechanochemical synthesis can be described according to reaction eq 3.

$$LiBH_4(s) + SrCl_2(s) \rightarrow Sr(BH_4)Cl(s) + LiCl(s) \quad (3)$$

Furthermore, observation of a small amount of $Sr(BH_4)_2$ indicates that the reaction shown in eq 4 occurs as a minor side reaction.

$$2LiBH_4(s) + SrCl_2(s) \rightarrow Sr(BH_4)_2(s) + 2LiCl(s) \quad (4)$$

Comparing the stoichiometry of reaction eq 4 ($2LiBH_4$:$SrCl_2$) to the sample composition ($LiBH_4$:$SrCl_2$) also explains why no $LiBH_4$ is observed, while some unreacted $SrCl_2$ (18.5(4) mol %, 31.5(6) wt%) remains in the sample after ball milling.

As the content of $LiBH_4$ in the starting composition is increased to $LiBH_4$:$SrCl_2$ = 2:1 (sample C), mechanochemical synthesis yields higher amounts of $Sr(BH_4)_2$, LiCl and two unidentified compounds, denoted **2** and **3** (see Figure 1). Hence, reaction eq 4 is occurring to a high extent. The unidentified compounds, **2** and **3**, have both been indexed in monoclinic unit cells, i.e., *a* = 10.015(2) Å, *b* = 5.811(2) Å, *c* = 8.666(3) Å, and β = 93.90(2)° for **2** and *a* = 10.726(4) Å, *b* = 6.832(3) Å, *c* = 7.251(3) Å, and β = 101.24(3)° for **3**. Le Bail fitting suggests space groups $P2/m$ and $P2_1/m$ for **2** and **3**, respectively. Increasing the content of $LiBH_4$ in the starting composition further, i.e., $LiBH_4$:$SrCl_2 \geq$ 3:1 (samples D and E), results in a significant decrease in the yield of $Sr(BH_4)_2$ and **2**, and for the sample of $LiBH_4$−$SrCl_2$ in a molar ratio of 4:1 (sample E) these compounds are not formed and only diffraction from **3**, LiCl, and unreacted $SrCl_2$ is observed (see Table 1 and Figure 2). The fact that unreacted $SrCl_2$ is present in all samples, while no diffraction from $LiBH_4$ is observed even in the samples of highest $LiBH_4$:$SrCl_2$ ratio, might suggest that $LiBH_4$ is consumed to a higher extent than by the metathesis shown in eq 4. Hence, formation of **2** and **3** possibly consumes $LiBH_4$. The decreasing yield of $Sr(BH_4)_2$ upon increasing $LiBH_4$ content in the starting composition might indicate that **2**

dx.doi.org/10.1021/ic400862s | *Inorg. Chem.* 2013, 52, 10877−10885

and **3** are lithium strontium borohydrides, i.e., $Li_xSr(BH_4)_{2+x}$ formed by an addition reaction between $Sr(BH_4)_2$ and $xLiBH_4$. Furthermore, sample compositions after milling suggest that x in $Li_xSr(BH_4)_{2+x}$ is higher for **3** than for **2**, since **3** is formed in higher yields in samples of higher $LiBH_4$:$SrCl_2$ molar ratios.

Some chloride substitution in $Sr(BH_4)_2$ is found to occur from both synthesis methods, i.e., a solid solution $Sr(BH_4)_{2-x}Cl_x$ is formed. This effect is most pronounced in the ball-milled samples, where Rietveld refinements suggest substitution degrees ranging from 16 to 31 mol %. The substitution degree, x, decreases with decreasing amounts of $SrCl_2$ in the reaction mixture, i.e., $LiBH_4$:$SrCl_2$ = 1:1 (sample B) exhibits the highest Cl substitution in $Sr(BH_4)_{2-x}Cl_x$. For the sample prepared by solvent-mediated synthesis only 9.8 mol % Cl substitution is observed.

Crystal Structures of $Sr(BH_4)_2$ and $Sr(BH_4)Cl$. Strontium borohydride, $Sr(BH_4)_2$, crystallizes in an orthorhombic unit cell with space group symmetry *Pbcn* (see Table 2). The structural drawing of the strontium borohydride $Sr(BH_4)_2$ is shown in Figure 3. The basic building unit for the structure of $Sr(BH_4)_2$

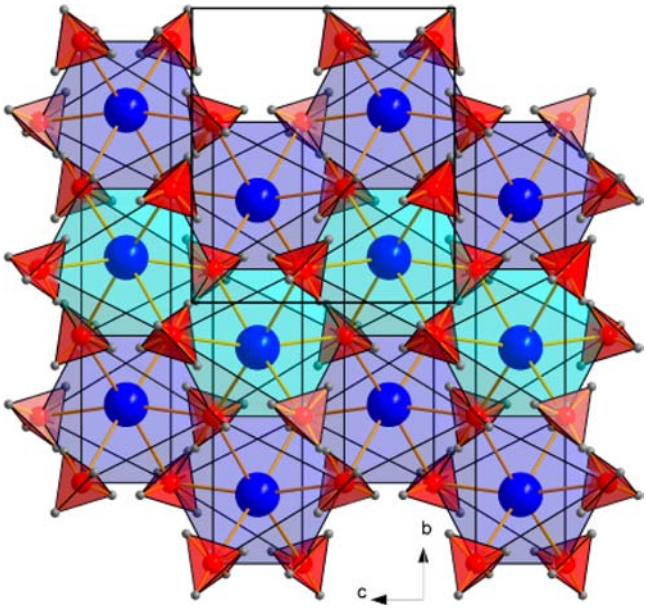

Figure 3. Crystal structures of $Sr(BH_4)_2$ (structure type α-PbO_2). Blue: Sr and red polyhedra, BH_4 units. For clarity, Sr−B coordinations are shown while Sr−H bonds are omitted. Basic building unit in $Sr(BH_4)_2$ is half-occupied brucite-like layer (011) of SrB_6 octahedra (blue) stacked in the *a*-axis direction. Second layer is shown in light blue.

is the borohydride anion BH_4^-, which is a regular tetrahedron. Strontium borohydride $Sr(BH_4)_2$ crystallizes in structure type α-PbO_2.[41] The structure is built from half-occupied brucite-like layers of slightly distorted $[Sr(BH_4)_6]$ octahedra stacked in the *a*-axis direction (Figure 3). The octahedra share two edges and all vertices with eight other octahedra in total. BH_4 units are coordinated by three Sr in a nonplanar triangle.

There are three different strontium−boron distances, each appearing twice within an octahedron either adjacent or opposite to each other; these are 2.96(3) (adjacent), 3.058(6) (opposite), and 3.12(3) Å (adjacent). These strontium−boron distances are consistent with the distance of 2.960 Å reported by Bremer et al. in $Sr(BH_4)_2$·2THF.[40] There are 3 B−Sr−B angles within 169.2(7)−173.9(7)° and 12 within 83.7(7)−97.3(7)°. The Sr−B−Sr angles within the nonplanar $[BSr_3]$ triangle range from 96.3(7)° to 129.9(9)°, and the distance of the B atom from the Sr plane is 0.36(3) Å. Hydrogen positions determined from antibump restraints in FOX suggest mixed bi- and tridentate coordination of the BH_4 units to Sr, i.e., four BH_4 units coordinating via the tetrahedral edge and two via the tetrahedral face. Thus, Sr seems to coordinate to 14 hydrogen atoms.

The novel strontium borohydride chloride, $Sr(BH_4)Cl$, crystallizes in an orthorhombic unit cell with space group symmetry *Pnma* (see Table 2). The structural drawing of the $Sr(BH_4)Cl$ viewed approximately along the *b* axis is shown in Figure 4a. The chloride/borohydride $Sr(BH_4)Cl$ is a stoichiometric, ordered compound with structure type $Sr(OH)_2$.[42] The same structure type was reported for HT-$SrBr_2$ and metastable SrI_2; however, it was later discovered that both compounds were hydrated, i.e., SrX_2·H_2O, X = Br and I. The fact that the structure of $SrCl_2$ is not preserved is likely due to incorporation of the BH_4^- anions, which is significantly larger than Cl^-, facilitating an expansion of the structure likely to cause structural rearrangement. The $Sr(BH_4)Cl$ structure is built from (011) layers of edge-sharing slightly distorted $[Sr(BH_4)_3Cl_4]$ monocapped trigonal prisms stacked in the *a*-axis direction (Figure 4b). Each prism shares eight edges and one vertex with nine other polyhedra in total. The BH_4 units keep the coordination by three Sr in a nonplanar triangle also found in $Sr(BH_4)_2$. Cl atoms coordinate to four Sr atoms in a distorted tetrahedral fashion similar to the coordination in cubic strontium chloride.[43] The Sr−Cl distances ranging from 2.95(1) to 3.03(1) Å are also similar to those in $SrCl_2$ of 3.019 Å. Sr−B distances are within 2.92(1)−2.93(1) Å, which is similar to those found in $Sr(BH_4)_2$. Sr−Cl−Sr angles cover a relatively wide range from 99.06(1)° to 136.9(1)°, while the Sr−B−Sr angles are within 103.97(1)−109.74(1)°. The distance of the B atom from the Sr plane in the $[BSr_3]$ trigonal coordination is 1.051(3) Å.

Table 3 lists the coordination numbers of Sr (CN(Sr)) within the series of strontium halides[43−49] as well as the anionic radii of the halides and the BH_4^- anion.[50,51] Anionic radii increase as $r(F^-) < r(Cl^-) < r(Br^-) < r(BH_4^-) < r(I^-)$. By comparing these values it becomes clear that CN(Sr) within the strontium borohydrides is not only determined by the anionic size, as that would imply a coordination between those in SrI_2 and $SrBr_2$, i.e., between 7 and 8. The lower CN(Sr) of 6 in $Sr(BH_4)_2$ reflects that the H−H repulsive forces between neighboring BH_4^- anions play a significant role for the structural topology. For $Sr(BH_4)Cl$ the coordination number of strontium is 7, which indicates that the presence of Cl in the coordination sphere somewhat reduces the H−H repulsive forces.

Raman Spectroscopy. Raman spectra of $Sr(BH_4)_2$ (sample A) are shown in Figure 5. For comparison, the Raman spectra of α-$Ca(BH_4)_2$ is also shown. The B atom in the structure of $Sr(BH_4)_2$ is located on a general position (8*d*) with site symmetry 1. Thus, there are no symmetry elements apart from the identity associated with the local symmetry of the BH_4^- anion. Consequently, the BH_4^- anion has point group *C1* and all of the $3N - 6 = 9$ vibrational modes would be expected to have *A*-type symmetry.

The strongest Raman signal for $Sr(BH_4)_2$, observed around 2300 cm^{-1}, is assigned to symmetric B−H stretching mode, υ_1. The other strong signal in the B−H stretching region is assigned to the asymmetric B−H stretching, υ_3 observed at

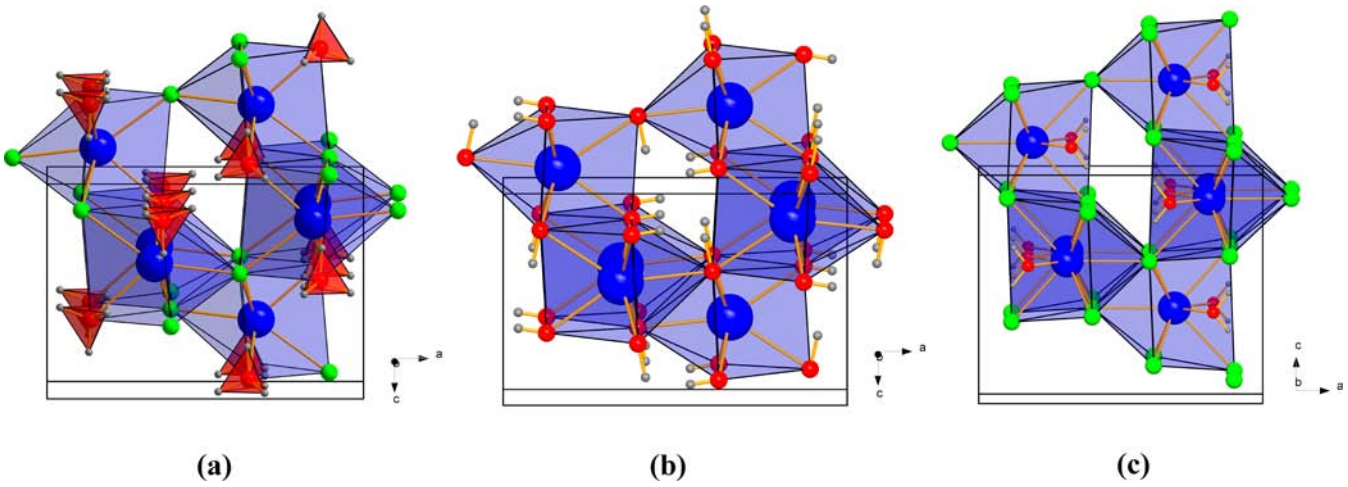

Figure 4. Crystal structure of $Sr(BH_4)Cl$ (a) shown along the *b* axis: blue, Sr; green, Cl; red polyhedra, BH_4 units. Basic building unit is (011) layer of an edge-sharing $Sr(BH_4)_3(Cl)_4$ monocapped trigonal prism (light) stacked in the *a*-axis direction. Structures of $Sr(OH)_2$ (b) and $SrBr_2{\cdot}H_2O$ (c) are shown for comparison.

Table 3. Anionic Radius of the Halides and the BH_4^- Anion[50,51] (top) and Comparison of Structure Types, Space Groups, Strontium Coordination Number (CN(Sr)), and Geometry for a Series of Strontium Halides[43−49] and $Sr(BH_4)_2$ and $Sr(BH_4)Cl$[a]

anion	F^-	Cl^-	Br^-	BH_4^-	I^-
radius (Å)	1.33	1.81	1.96	2.05	2.20

compound	structure type	space group	CN(Sr)[b]	Sr coordination	ref
$Sr(BH_4)_2$	α-PbO_2	*Pbcn*	6	octahedron	This work
$Sr(BH_4)Cl$	$Sr(OH)_2$	*Pnma*	7	monocapped trigonal prism $[Sr(BH_4)_3Cl_4]$	This work
SrF_2 $SrCl_2$	CaF_2	*Fm*-3*m*	8	cube	43 44
$SrBr_2$	$SrBr_2$	*P*4/*n*	8	square antiprism	45
SrI_2	SrI_2	*Pbca*	7	monocapped trigonal prism	46
high pressure/temperature SrI_2	$PbCl_2$	*Pnma*	9	tricapped trigonal prism	47
$SrBr_2{\cdot}H_2O$, $SrI_2{\cdot}H_2O$	$BaCl_2{\cdot}H_2O$	*Pnma*	9	tricapped trigonal prism $[SrX_7(H_2O)_2]$, X = Br or I	48, 49

[a]Note the low CN(Sr) of 6 in $Sr(BH_4)_2$, which reflects that not only the anionic radius but to a high extent also the H−H repulsive forces are important for coordination in $Sr(BH_4)_2$ and $Sr(BH_4)Cl$. [b]In the coordination number (CN) a Sr−BH_4 coordination counts as 1.

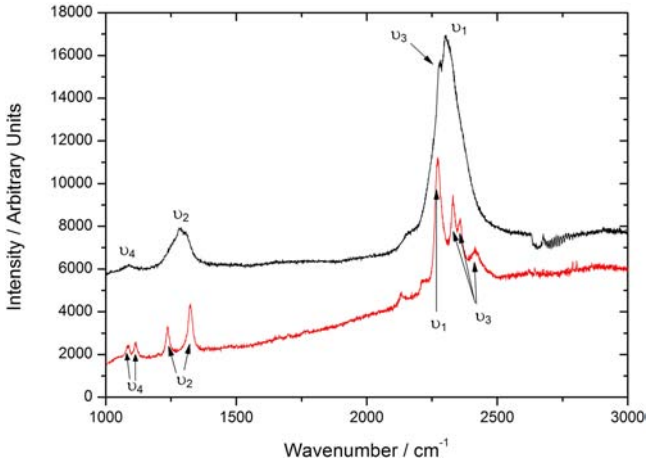

Figure 5. Raman spectra measured at RT for $Sr(BH_4)_2$ prepared by solvent-mediated synthesis (black, sample A) and α-$Ca(BH_4)_2$ (red).

2280 cm^{-1}. In other borohydrides, υ_3 vibrations have been observed on either or both sides of υ_1; hence, the presence of υ_3 on the opposite side of υ_1 compared to $Ca(BH_4)_2$ is not particularly significant. Comparison with the Raman spectrum of $Ca(BH_4)_2$[52] and the alkali metal borohydrides[53] would suggest that the symmetric B−H bond bending vibrations, υ_2, are around 1280 cm^{-1}, and the asymmetric B−H bond bending vibrations, υ_4, are around 1090 cm^{-1}.

The fact that no significant splitting is observed for the stretching mode confirms the framework topology of the $Sr(BH_4)_2$ structure containing only bridging BH_4. Similar observations have been reported for other framework structures such as α-$Mg(BH_4)_2$ and $Mn(BH_4)_2$.[30,54,55] In contrast, structures containing isolated anions or polymeric units exhibit several modes within the stretching region due to the presence of terminal BH_4 units, e.g., for $LiZn_2(BH_4)_5$ stretching modes for both the bridging and terminal B−H units within the complex anion $[Zn_2(BH_4)_5]^-$ are observed, giving rise to four modes between 2100 and 2458 cm^{-1}.[18,56] Furthermore, observation of the relatively strong bending mode at 1280 cm^{-1} confirms the presence of tridentate BH_3−Sr bonding.[57,58] This band is comparable to the bands observed around 1200 cm^{-1} for $MSc(BH_4)_4$ (M = Li, Na, or K) and $NaY(BH_4)_2Cl_2$ in which the BH_4 units also act as η^3-ligands.[13,15,16,59]

No peaks are observed corresponding to either THF or diethyl ether, which is likely present in compound **1** in sample A. This may be due to the small amount of **1** in the sample compared to $Sr(BH_4)_2$ and LiCl.

dx.doi.org/10.1021/ic400862s | *Inorg. Chem.* 2013, 52, 10877−10885

Decomposition Analysis by in-Situ SR-PXD. Thermal decomposition of $Sr(BH_4)Cl$ was investigated by in-situ SR-PXD for the ball-milled sample of $LiBH_4$−$SrCl_2$ in a molar ratio of 1:1 (sample B), shown in Figure 6. From RT to ∼170 °C

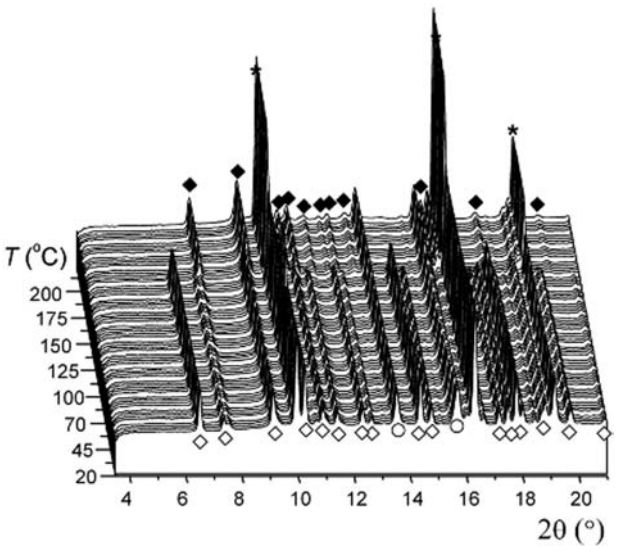

Figure 6. In-situ SR-PXD data for a sample containing $Sr(BH_4)Cl$ ($LiBH_4$−$SrCl_2$, 1:1, sample B) measured from RT to 230 °C, $\Delta T/\Delta t$ = 1 °C/min (BM01A, ESRF, λ = 0.832117 Å): (◊) $Sr(BH_4)Cl$, (○) LiCl, (*) $SrCl_2$, (♦) $Sr(BH_4)_2$.

diffraction from $Sr(BH_4)Cl$, $SrCl_2$, and LiCl is observed. At ∼170 °C all diffraction from $Sr(BH_4)Cl$ vanishes simultaneously with formation of $Sr(BH_4)_2$ and $SrCl_2$. Hence, $Sr(BH_4)Cl$ dissociates according to the reaction shown in eq 5.

$$Sr(BH_4)Cl(s) \rightarrow Sr(BH_4)_2(s) + SrCl_2(s) \quad (5)$$

For the remainder of the experiment, i.e., in the temperature range from 170 to 230 °C, no significant changes in the diffraction from $Sr(BH_4)_2$ and $SrCl_2$ are observed.

Thermal decomposition of $Sr(BH_4)_2$ is investigated by in-situ SR-PXD for samples A, C, and D. These data also provide some insight into the behavior of the unknown compounds observed after solvent-mediated synthesis (**1**) and ball milling (**2** and **3**). For the sample prepared by solvent-mediated synthesis (sample A) diffraction from $Sr(BH_4)_2$ and **1** is observed from RT to 100 °C, where **1** vanishes simultaneously with an increase in the diffracted intensity from $Sr(BH_4)_2$. Hence, it underlines that **1** might be a strontium borohydride solvate, i.e., $Sr(BH_4)_2{\cdot}nEt_2O$ or $Sr(BH_4)_2{\cdot}n$THF. From 100 to 350 °C only diffraction from $Sr(BH_4)_2$ and a small amount of LiCl is observed. Between 200 and 300 °C, $Sr(BH_4)_2$ seems to be annealed and the Bragg peaks become sharper. At 350 °C diffraction from $Sr(BH_4)_2$ disappears and a new set of broad peaks is observed. This set of Bragg peaks was indexed in an orthorhombic unit cell with a = 18.4808(9) Å, b = 5.7526(2) Å, c = 14.3600(6) Å, and V = 1526.65(11) Å^3.

For the ball-milled sample of $LiBH_4$−$SrCl_2$ in a molar ratio of 3:1 (sample D), diffraction from **3**, $SrCl_2$, LiCl, and a small amount of $Sr(BH_4)_2$ is observed at RT (see Figure S1, Supporting Information). Upon heating to ∼125 °C, diffraction from **3** vanishes simultaneously with formation of $Sr(BH_4)_2$. It should also be noted that the unknown compound, **2**, is observed to decompose at ∼105 °C (from data of sample C). The relatively low decomposition temperature of **2** and **3** indicates that these might be borohydrides, since chloride salts are expected to be significantly more stable. Furthermore, formation of $Sr(BH_4)_2$ from decomposition of **3** suggests that this is entailed in the structure of **3**, i.e., it might be a $Li_xSr(BH_4)_{2+x}$. After decomposition of $Sr(BH_4)_2$ diffraction, most likely from several compounds, is observed. The diffraction shows significant "spotty" character, likely due to the fact that these compounds form from a melt, causing formation of small single crystals rather than a powder. This complicates data analysis, and these compounds have not been identified. As the temperature reaches ∼410 °C slow formation of SrB_6 is initiated as well as formation of an unknown decomposition product, which has been indexed in an orthorhombic cell (a = 7.1156 Å, b = 6.8124 Å, and c = 5.3032 Å). Formation of SrB_6 might suggest formation of SrH_2 (e.g., $3Sr(BH_4)_2 \rightarrow SrB_6 + 2SrH_2 + 10\ H_2$), which is stable at T < 675 °C.[60] However, diffraction from SrH_2 has not been observed in any of the conducted experiments. From these observations it is evident that decomposition of $Sr(BH_4)_2$ is relatively complex and cannot be deduced in detail from the present data. Furthermore, higher boranes, e.g., $SrB_{12}H_{12}$, might form as decomposition intermediates, as suggested for other borohydrides including $Ca(BH_4)_2$ and $LiBH_4$.[61,62] The existence of $SrB_{12}H_{12}{\cdot}7H_2O$ has been previously reported.[63] The high stability of SrB_6 may hamper reversible hydrogen storage in $Sr(BH_4)_2$.

CONCLUSIONS

The synthesis, crystal structure, and thermal decomposition have been investigated for two novel metal borohydrides, $Sr(BH_4)_2$ and $Sr(BH_4)Cl$. The former was obtained from a metathesis reaction between MBH_4 (M = Li or Na) and $SrCl_2$ by solvent-mediated as well as mechanochemical synthesis, i.e., ball milling, while $Sr(BH_4)Cl$ was only obtained by ball milling $LiBH_4$−$SrCl_2$ in a molar ratio of 1:1. The latter compound forms from an addition reaction between $Sr(BH_4)_2$ and $SrCl_2$. Furthermore, three additional compounds were discovered: **1** is most likely a strontium borohydride solvate, while **2** and **3** may be $Li_xSr(BH_4)_{2+x}$.

$Sr(BH_4)_2$ consists of a framework of slightly distorted $[Sr(BH_4)_6]$ octahedra stacked in half-occupied brucite-like layers along the a axis. The $Sr(BH_4)Cl$ framework is built from (011) layers of edge-sharing slightly distorted $[Sr(BH_4)_3Cl_4]$ monocapped trigonal prisms stacked along the a axis. Comparison of these novel borohydride structures to a series of strontium halides reveals the large effect of H−H repulsive forces on the strontium coordination numbers.

Investigation of the thermal decomposition by in-situ SR-PXD showed that $Sr(BH_4)Cl$ dissociates to $Sr(BH_4)_2$ and $SrCl_2$ at ∼170 °C, while $Sr(BH_4)_2$ decomposes at ∼350 °C with formation of multiple decomposition intermediates and SrB_6 as the final decomposition product. The fact that SrB_6 was observed among the final decomposition products may suggest that boron is kept in the solid state during hydrogen release from $Sr(BH_4)_2$, which is a prerequisite for safe, reversible hydrogen storage.

ASSOCIATED CONTENT

Supporting Information

Figure of in-situ SR-PXD data of a ball-milled sample of $LiBH_4$−$SrCl_2$ (3:1); tables of atomic coordinates of $Sr(BH_4)_2$, $Sr(BH_4)_2$, and $Sr(BH_4)Cl$. This material is available free of charge via the Internet at http://pubs.acs.org.

AUTHOR INFORMATION

Corresponding Author

*Phone: 617-253-5308. E-mail: dorthe@mit.edu.

Notes

The authors declare no competing financial interest.

ACKNOWLEDGMENTS

D.B.R. and T.R.J. thank the Danish Research Council for Nature and Universe (Danscatt), the Danish National Research Foundation (Centre for Materials Crystallography), the Danish Strategic Research Council (HyFillFast), and the Carlsberg Foundation for funding. E.A.N. acknowledges EPSRC and STFC for funding. We are also grateful to SNBL, ESRF, and MAX-lab for the provision of beam time. This work was supported by the Swiss National Science Foundation.

REFERENCES

(1) Eberle, U.; Felderhoff, M.; Schüth, F. *Angew. Chem.* **2009**, *121*, 6732−6757.

(2) Schlapbach, L. *Nature* **2009**, *460*, 809−811.

(3) Orimo, S.; Nakamori, Y.; Eliseo, J. R.; Zuttel, A.; Jensen, C. M. *Chem. Rev.* **2007**, *107*, 4111−4132.

(4) Rude, L. H.; Nielsen, T. K.; Ravnsbæk, D. B.; Bösenberg, U.; Ley, M. B.; Richter, B.; Arnbjerg, L. M.; Dornheim, M.; Filinchuk, Y.; Besenbacher, F.; Jensen, T. R. *Phys. Status Solidi A* **2011**, *208*, 1754−1773.

(5) Züttel, A.; Wenger, P.; Rentsch, S.; Sudan, P.; Mauron, Ph.; Emmenegger, Ch. *J. Power Sources* **2003**, *118*, 1−7.

(6) Ravnsbæk, D. B.; Sørensen, L. H.; Filinchuk, Y.; Besenbacher, F.; Jensen, T. R. *Angew. Chem., Int. Ed.* **2012**, *51*, 3582−3586.

(7) Nickels, E. A.; Jones, M. O.; David, W. I. F.; Johnson, S. R.; Lowton, R. L.; Sommariva, M.; Edwards, P. P. *Angew. Chem., Int. Ed.* **2008**, *47*, 2817−2819.

(8) Ĉerný, R.; Filinchuk, Y. *Z. Kristallogr.* **2011**, *226*, 882−891.

(9) Ley, M. B.; Ravnsbæk, D. B.; Filinchuk, Y.; Lee, Y.-S.; Janot, R.; Cho, Y. W.; Skibsted, J.; Jensen, T. R. *Chem. Mater.* **2012**, *24*, 1654−1663.

(10) Ley, M. B.; Boulineau, S.; Janot, R.; Filinchuk, Y.; Jensen, T. R. *J. Phys. Chem. C* **2012**, *116*, 21267−21276.

(11) Ĉerný, R.; Ravnsbæk, D. B.; Schouwink, P.; Filinchuk, Y.; Penin, Y.; Teyssier, J.; Smrčok, L.; Jensen, T. R. *J. Phys. Chem. C* **2012**, *116*, 1563−1571.

(12) Schouwink, P.; D'Anna, V.; Ley, M. B.; Daku, L. M. L.; Richter, B.; Jensen, T. R.; Hagemann, H.; Ĉerný, R. *J. Phys. Chem. C* **2012**, *116*, 10829−10840.

(13) Hagemann, H.; Longhini, M.; Kaminski, J. W.; Wesolowski, T. A.; Ĉerný, R.; Penin, N.; Sørby, M. H.; Hauback, B. C.; Severa, G.; Jensen, C. M. *J. Phys. Chem. A* **2008**, *112*, 7551−7555.

(14) Hwang, S. -J.; Bowman, R. C., Jr.; Reiter, J. W.; Rijssenbeek, J.; Soloveichik, G. L.; Zhao, J.-C.; Kabbour, H.; Ahn, C. C. *J. Phys. Chem. C* **2008**, *112*, 3164−3169.

(15) Ĉerný, R.; Severa, G.; Ravnsbæk, D. B.; Filinchuk, Y.; d'Anna, V.; Hagemann, H.; Haase, D.; Jensen, C. M.; Jensen, T. R. *J. Phys. Chem. C* **2010**, *114*, 1357−1364.

(16) Ĉerný, R.; Ravnsbæk, D. B.; Severa, G.; Filinchuk, Y.; d'Anna, V.; Hagemann, H.; Haase, D.; Skibsted, J.; Jensen, C. M.; Jensen, C. M. *J. Phys. Chem. C* **2010**, *114*, 19540−19549.

(17) Ravnsbæk, D.; Filinchuk, Y.; Cerenius, Y.; Jakobsen, H. J.; Besenbacher, F.; Skibsted, J.; Jensen, T. R. *Angew. Chem., Int. Ed.* **2009**, *48*, 6659−6663.

(18) Ravnsbæk, D. B.; Frommen, C.; Reed, D.; Filinchuk, Y.; Sørby, M.; Hauback, B. C.; Jakobsen, H. J.; Book, D.; Besenbacher, F.; Skibsted, J.; Jensen, T. R. *J. Alloys Compd.* **2011**, *509*, S698−S704.

(19) Filinchuk, Y.; Chernyshov, D.; Dmitriev, V. *Z. Kristallogr.* **2008**, *223*, 649−659.

(20) Filinchuk, Y.; Richter, B.; Jensen, T. R.; Dmitriev, V.; Chernyshov, D.; Hagemann, H. *Angew. Chem.* **2011**, *123*, 11358−11362; *Angew. Chem., Int. Ed.* **2011**, *50*, 11162−11166.

(21) David, W. I. F.; Callear, S. K.; Jones, M. O.; Aeberhard, P. C.; Culligan, S. D.; Pohl, A. H.; Johnson, S. R.; Ryan, K. R.; Parker, J. E.; Edwards, P. P.; Nuttall, C. J.; Amieiro-Fonseca, A. *Phys. Chem. Chem. Phys.* **2012**, *14*, 11800−11807.

(22) Paskevicius, M.; Pitt, M.; Webb, C. J.; Sheppard, D. A.; Filsø, U.; Gray, E. M.; Buckley, C. E. *J. Phys. Chem. C* **2012**, *116*, 15231−15240.

(23) Hagemann, H.; Ĉerný, R. *Dalton Trans.* **2010**, *39*, 6006−6012.

(24) Huot, J.; Ravnsbæk, D. B.; Zhang, J.; Cuevas, F.; Latroche, M.; Jensen, T. R. *Prog. Mater. Sci.* **2013**, *58*, 30−75.

(25) Mikheeva, V. I.; Sizareva, A. S. *Zh. Neorg. Khim.* **1977**, *22*, 1706.

(26) Jensen, T. R.; Nielsen, T. K.; Filinchuk, Y.; Jørgensen, J.-E.; Cerenius, Y.; Mac. Gray, E.; Webb, C. J. *J. Appl. Crystallogr.* **2010**, *43*, 1456−1463.

(27) Hammersley, A. P.; Svensson, S. O.; Hanfland, M.; Fitch, A. N.; Häusermann, D. *High Pressure Res.* **1996**, *14*, 235−248.

(28) David, W. I. F.; Shankland, K.; van de Streek, J.; Pidcock, E.; Motherwell, W. D. S.; Cole, J. C. *J. Appl. Crystallogr.* **2006**, *39*, 910−915.

(29) Coelho, A. A. *TOPAS*; Academic Press: New York, 2004.

(30) Ĉerný, R.; Filinchuk, Y.; Hagemann, H.; Yvon, K. *Angew. Chem. Int, Ed.* **2007**, *46*, 5765−5767.

(31) Her, J.-H.; Stephens, P. W.; Gao, Y.; Soloveichik, G. L.; Rijssenbeek, J.; Andrus, M.; Zhao, J.-C. *Acta Crystallogr., Sect. B: Struct. Sci.* **2007**, *63*, 561−568.

(32) Miwa, K.; Aoki, M.; Noritake, T.; Ohba, N.; Nakamori, Y.; Towata, S.; Zuttel, A.; Orimo, S. *Phys. Rev. B: Condens. Matter* **2006**, *74*, 155122.

(33) Buchter, F.; Łodziana, Z.; Remhof, A.; Friedrichs, O.; Borgschulte, A.; Mauron, P.; Züttel, A.; Sheptyakov, D.; Barkhordarian, G.; Bormann, R.; Chlopek, K.; Fichtner, M.; Sorby, M. H.; Riktor, M. D.; Hauback, B. C.; Orimo, S. *J. Phys. Chem. B* **2008**, *112*, 8042.

(34) Hahn, T. *International Tables for Crystallography*; Springer for International Union of Crystallography: Dordrecht, The Netherlands, 2005; Vol. *A*.

(35) Larson, A. C.; Von Dreele, R. B. *Los Alamos National Laboratory Report LAUR* **1994**, 86−748.

(36) Boultif, A.; Louer, D. *J. Appl. Crystallogr.* **2004**, *37*, 724.

(37) Favre-Nicolin, V.; Ĉerný, R. *J. Appl. Crystallogr.* **2002**, *35*, 734.

(38) Rodrigues-Carvajal, J. *Physica B* **1993**, *192*, 55. For a more recent version, see: Rodríguez-Carvajal, J. Recent developments of the program FULLPRO; Commission on Powder Diffraction Newsletters (IUCr), Chester, England, 2001; Vol. 26, pp 12−19. The complete program and documentation can be obtained at http://www.iucr.org/__data/assets/pdf_file/0019/21628/cpd26.pdf.

(39) Spek, A. L. *PLATON*; University of Utrecht: The Netherlands, 2006.

(40) Bremer, M.; Nöth, H.; Thomann, M.; Schmidt, M. *Chem. Ber.* **1995**, *128*, 455−460.

(41) Zaslavskii, A. I.; Kondrashev, Yu. D.; Tolkachev, S. S. *Dokl. Akad. Nauk SSSR* **1950**, *75*, 559−561.

(42) (a) Partin, D. E.; O'Keeffe, M. *J. Solid State Chem.* **1995**, *119*, 157−160. (b) Engelen, B.; Kellersohn, T.; Kuske, P.; Lutz, H. D. *Z. Anorg. Allg. Chem.* **1988**, *566*, 49−54.

(43) Ott, H. *Z. Kristallogr. Krist.* **1926**, *63*, 222−230.

(44) Greis, O.; Petzel, T. *Z. Anorg. Allg. Chem.* **1974**, *403*, 1−96.

(45) Sass, R. L.; Brackett, T. E.; Brackett, E. B. *J. Phys. Chem.* **1963**, *67*, 2862−2863.

(46) Hodorowicz, S. A.; Eick, H. A. *J. Solid State Chem.* **1983**, *46*, 313−320.

(47) Liu, G.; Eick, H. A. *J. Less-Common Met.* **1989**, *156*, 237−245.

(48) Dyke, M.; Sass, R. L. *J. Phys. Chem.* **1964**, *68*, 3259−3262.

(49) Lutz, H. D.; Buchmeier, W.; Engelen, B. *Acta Crystallogr., Sect. B* **1987**, *43*, 71−75.

(50) Lide, D. R. *CRC Handbook of Chemistry and Physics*, 88th ed.; CRC: Boca Raton, FL, 2007.

(51) Barron, A. R.; Hursthouse, M. B.; Motevalli, G.; Wilkinson, G. *Chem. Commun.* **1986**, 81−82.
(52) Fichtner, M.; Chłopek, K.; Longhini, M.; Hagemann, H. *J. Phys. Chem. C* **2008**, *112*, 11575.
(53) Orimo, S.; Nakamori, Y.; Zuttel, A. *Mater. Sci. Eng.* **2004**, *B104*, 51.
(54) Filinchuk, Y.; Ĉerný, R.; Hagemann, H. *Chem. Mater.* **2009**, *21*, 925−933.
(55) Ĉerný, R.; Penin, N.; Hagemann, H.; Filinchuk, Y. *J. Phys. Chem. C* **2009**, *113*, 9003−9007.
(56) Ĉerný, R.; Kim, K. C.; Penin, N.; D'Anna, V.; Hagemann, H.; Sholl, D. S. *J. Phys. Chem. C* **2010**, *114*, 19127−19133.
(57) Marks, T. J.; Kolb, J. R. *Chem. Rev.* **1977**, *77*, 263−293.
(58) Reed, D.; Book, D. *Curr. Opin. Solid State Mater. Sci.* **2011**, *15*, 62−72.
(59) Ravnsbæk, D. B.; Ley, M. B.; Lee, Y.-S.; Hagemann, H.; D'Anna, V.; Cho, Y. W.; Filinchuk, Y.; Jensen, T. R. *Int. J. Hydrogen Energy* **2012**, *37*, 8428−8438.
(60) Grochala, W.; Edwards, P. P. *Chem. Rev.* **2004**, *104*, 1283−1315.
(61) Wang, L.-L.; Graham, D. D.; Robertson, I. M.; Johnson, D. D. *J. Phys. Chem. C* **2009**, *113*, 20088.
(62) Her, J.-H.; Yousufuddin, M.; Zhou, W.; Jalisatgi, S. S.; Kulleck, J. G.; Zan, J. A.; Hwang, S.-J.; Bowman, R. C, Jr.; Udovic, T. J. *Inorg. Chem.* **2008**, *47*, 9757.
(63) Solntsev, K. A.; Kuznetsov, N. T.; Kol'ba, L. N.; Agre, V. M.; Ponomarev, V. I. *Russ. J. Inorg. Chem.* **1977**, *22*, 313.